Ion temperature measurement on tokamak Golem

Author: Dario Cipciar **Date:** 6.4.2021

Faculty of Science, Masaryk University, Department of electronics

---

1. Abstract

We attempted to systematically measure ion temperatures on tokamak Golem using a swept ball-pen probe. We have performed multiple discharges with different parameters and radial positions in order to find optimal conditions for measurement with ball-pen probe.

2. Experimental setup and data preparation

In this experimental campaign we have performed measurements of ion temperature (T_i) and electron temperature (T_e) using stationary electric probes at different radial positions during discharge in Ohmic (OH) regime. The tokamak was purged by a glow discharge in helium and was well prepared for T_i measurement. Data Acquisition System (DAS) was set to sampling frequency of 12.5 MHz. Coaxial cables had length of 8 m.

2.1. Experimental set-up and data preparation

Discharge parameters were set to:

Voltage on condenser batteries powering toroidal magnetic field coils: $U_{Bt} = 1200$ V,

Current drive field source voltage: $U_{CD} = 400$ V,

Current drive trigger delay: $\tau_{CD} = 2000$ ms,

Requested gas pressure: $p = 10$ mPa.

Probe tip position: $R = 70, 67.5, 65, 60, 55$ mm.

The ball-pen probe (BPP) was biased with voltage of -150 to +150 V, at a sweeping frequency of 50 kHz or 10 kHz. The Langmuir probe was in a floating regime. The schematic is shown on Fig. 1 The range of oscilloscope was set to 1 V. The discharge plasma parameters are shown on Fig. 2. The measured raw probe data are shown on Fig. 3.

Very large stray currents were observed due to high sweeping frequency spreading through 8 m long coaxial cable. Signal clean-up procedure is applied to remove stray current. We use lowpass filter in order to remove structures with much higher frequency than the voltage sweeping frequency. The study of non-linear IV-characteristics with a sweeping frequency of E.g. 50 kHz requires that we measure also higher harmonics of this frequency. The upper bandwidth limit was set to 370 kHz, which allows to

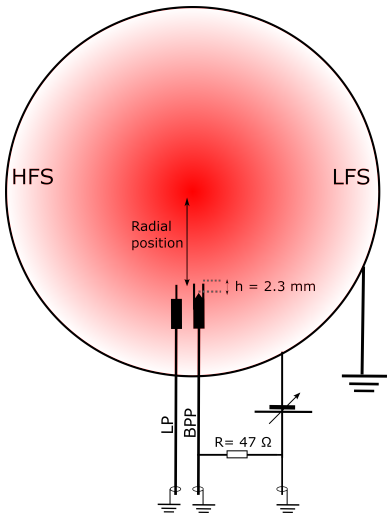

Figure 1: Simplified schematic of a probe setup. View of a tokamak plasma cross-section.

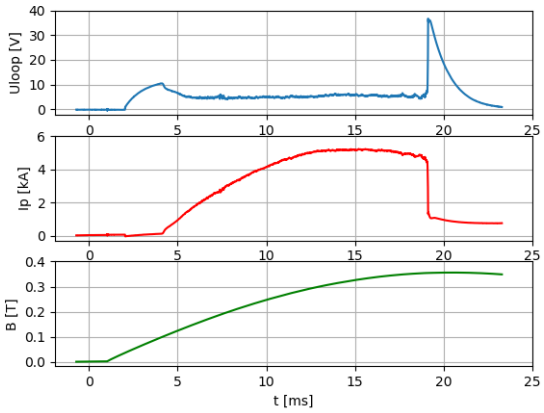

Figure 2: Plasma parameters, shot: 35366

measure 7 harmonics. Lowpass filter alone will not remove the capacitive current. We can model the stray current as

$$I = C\frac{dU}{dt} + \text{offset}. \tag{1}$$

The capacity C can be obtained from slope of a linear dependency of the voltage derivative to current measured. Reconstructed stray current and offset is than subtracted from measured signal. Example of such signal clean-up procedure is shown on Figures 3, where the capacitive current is reconstructed and removed. On the same figure we can see, that some stray current, although 100x lower in amplitude, still remains. This current shown in red on Fig. 3 is in comparison to previously reconstructed current shifted in phase by $\pi/2$. We can repeat the same signal clean-up procedure, as shown on Fig. 4, however this time we need to compensate for the phase shift (shown on upmost sub-figure). The second capacitive current is removed and as shown on Fig. 5 the lowpass filter is applied. We can see that the amplitude of stray current decreased to 1/200 of it's initial amplitude.

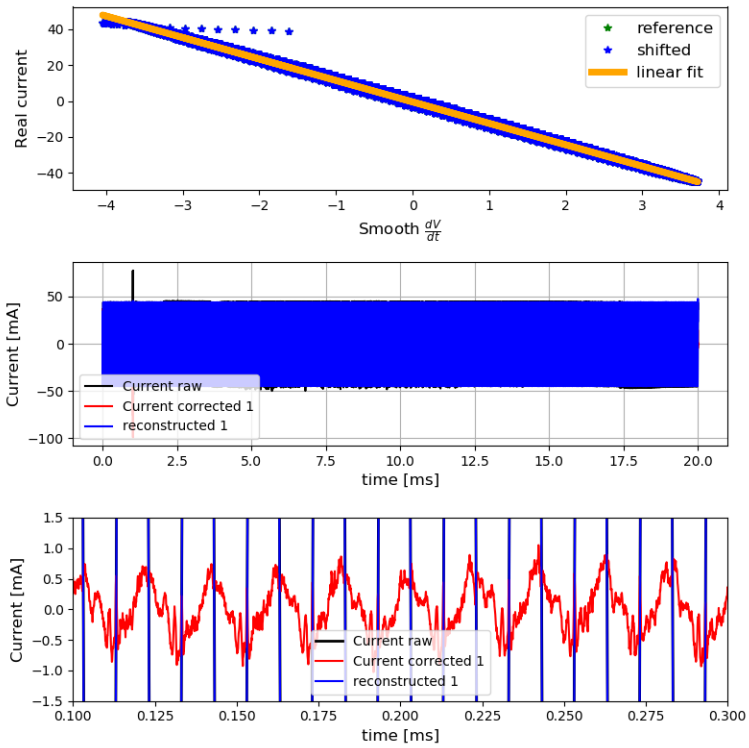

Figure 3: First stray current reconstruction and removal, shot: 35346

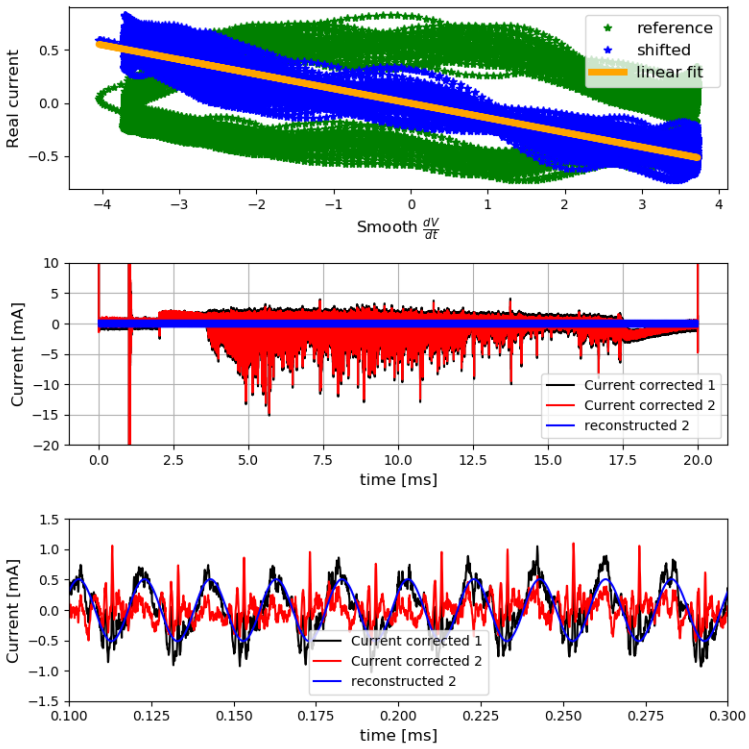

Figure 4: Second (phase shifted) stray current reconstruction and removal, shot: 35346

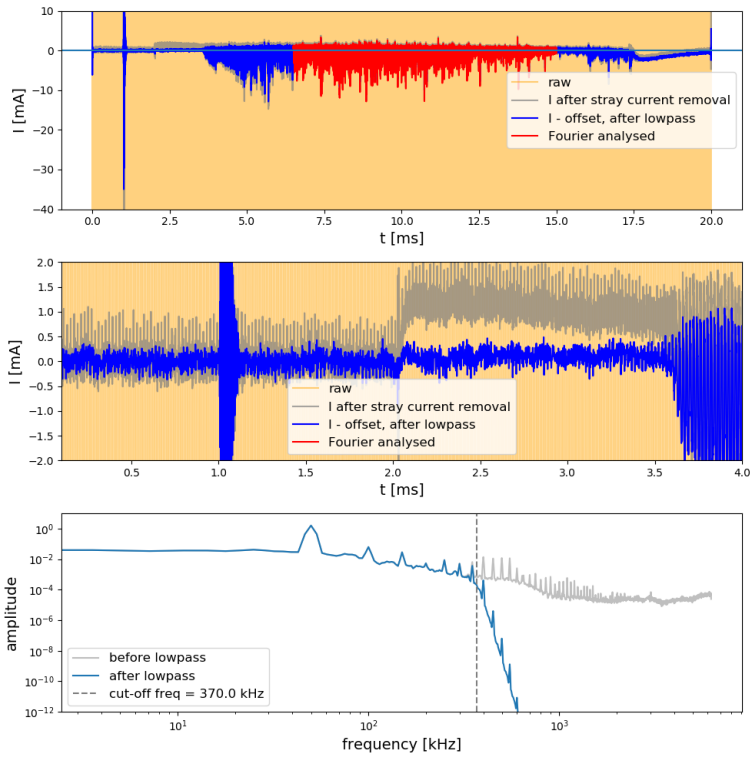

Figure 5: Removal of an offset caused by interference with other diagnostics (probably through grounding). The offset signal was obtained from vacuum discharge # 35353. Further lowpass filter and a fourier analysis of signal is shown, shot: 35346

I-V characteristics can be fitted from the plasma potential V_p using a 4-parameter fit. Since magnitude of the magnetic field was changing during the whole discharge we have used the unweighted method for fitting the I-V characteristics. The formula used for 4-parameter fitting is:

$$I(V) = \exp(\alpha_\mathrm{BPP}) I^+_\mathrm{sat}[1 + R(V - \Phi)] - I^+_\mathrm{sat} \exp((\Phi - V)/T_\mathrm{i}). \tag{2}$$

The fitting parameters obtained are the ion temperature (T_i), plasma potential (Φ), ion saturation current (I^+_sat) and linear increase of electron current is described by slope (R).

3. Calculation of the coefficient α_BPP

The BPP was biased with voltage of -150 to +150 V, at a sweeping frequency of 10 kHz.

At first the I-V characteristics needs to be normalized to ion saturation current (I^+_sat). The normalization is crucial for removing the effects of the plasma density fluctuations during the discharge and enables us to compare the results of multiple discharges. The value of I^+_sat can be obtained if we perform a 4-parameter fit of the ion-branch of the BPP I-V characteristics. The ion branch of BPP characteristics is measured when the bias voltage is below the plasma potential. We found an analytical function describing the ion-branch of BPP given as:

$$I = I^+_\mathrm{sat}[1 + K(V - \Phi^\mathrm{BPP}_\mathrm{fl})] - I^+_\mathrm{sat} \exp\left(\frac{(V - \Phi^\mathrm{BPP}_\mathrm{fl})}{T_\mathrm{e}}\right). \tag{3}$$

The 4-parameter fit is capable of accounting for the possible sheath expansion effect causing the linear growth of the ion saturation current with a slope $\frac{\Delta I}{\Delta V} = K$.

After the estimation of saturation current the whole I–V characteristics can be normalized. The example of 4-parameter fit of the BPP ion branch and subsequent normalization to ion saturation current is shown on Fig. 6

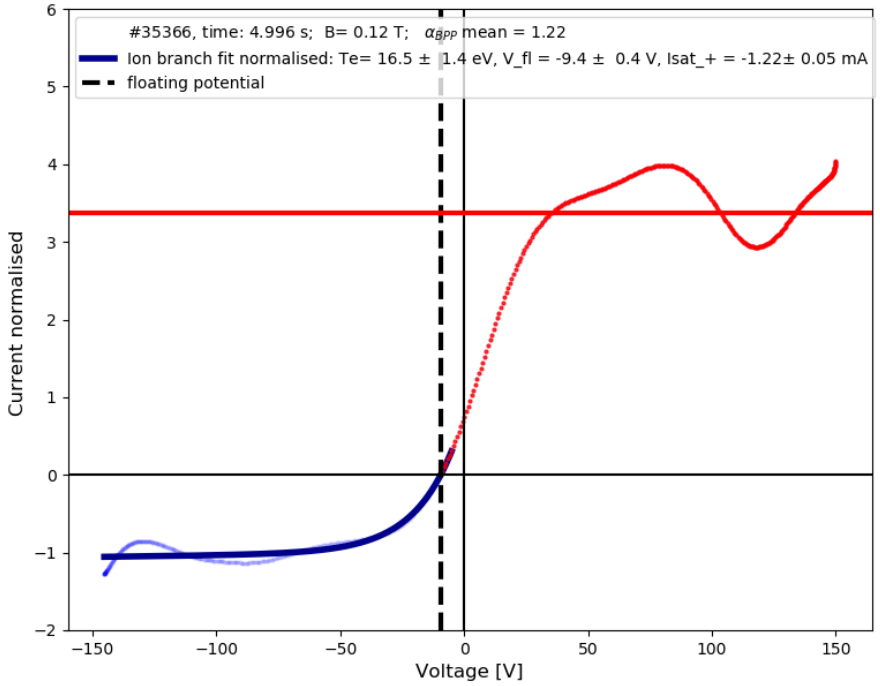

Figure 6: The 4-parameter fit (dark blue) of the BPP ion branch (light blue) 3 and subsequent normalization to ion saturation current. The red horizontal line (mean of saturated part of electron branch) is the first estimate of electron to ion saturation current ratio.

Secondly we need to estimate to estimate the electron saturation current from the electron branch of I-V. We approach the problem in a similar way. However, the electron branch tends to fluctuate on a much greater scale than the ion branch. In order to reduce the fluctuations it is reasonable to use an averaging method to receive more stable fits. We than repeat same process as discussed before, but this time for 10 single I-V characteristics. Each of the I-Vs is normalized to it's I^{+}_{sat}. These normalized I-V characteristics are than averaged into a single (slow) "bin-averaged" I-V characteristic over a period of 0.5 ms, with voltage bins of 10 V. This technique provides a robust approach to fitting and delivers stable parameters (see Fig. 7).

Now we can proceed to fitting of the bin-averaged I-V characteristics using a 4-parameter fitting formula. The analytical function describing the electron branch of BPP needs to be modified since the electron branch was normalized to ion saturation current. We receive:

$$I = \mathcal{R}[1 + K(V - \Phi)] - 1 \exp\left(\frac{\Phi - V}{T_{\mathrm{i}}}\right), \quad \text{where} \quad \mathcal{R} = \frac{\mathrm{I}^{-}_{\mathrm{sat}}}{\mathrm{I}^{+}_{\mathrm{sat}}}. \tag{4}$$

The ratio of electron to ion saturation current $\mathcal{R}$ is obtained directly as a parameter of the 4-parameter fit. The calibration coefficient is then $\alpha_{\mathrm{BPP}} = \ln(\mathcal{R})$. However, in order to increase the precision and stability of the fit, we estimate the plasma potential and fix the parameter Φ in the equation 4. The plasma potential of the ball-pen probe is located in the inflection point.

However, the normalized 4-parameter fit of the electron branch is not correct when $I^-_{\mathrm{sat}} \gg I^+_{\mathrm{sat}} = 1$. The reason for this assumption is the basic requirement for BPP to function, the strong magnetic field. In a very low magnetic field the Larmor radius **??** of electrons increases until the electrons start to ignore the shielding tube and transport to the collector the same way ions do. In this case the BPP functions as a simple Langmuir probe. The BPP operating as a Langmuir probe is undesirable. We can thus only estimate the electron saturation current using a mean value from a chosen (saturation) interval (+80 V; +140 V) of the electron branch. This estimation of I^-_{sat} is later used for confirmation of validity of 4-parameter fit 4. We have applied a condition: $I^-_{\mathrm{sat}} < 4$. When this condition is satisfied we can fit the electron branch and obtain the value of $\mathcal{R}$ as a fitting parameter. The received mean values of saturation interval are only an approximate estimation of the ratio and are not used for calculation of the final α_{BPP}.

In order to construct the dependency of the coefficient on magnetic field strength, the above described process is run over the whole discharge. Extremely unsaturated I-V characteristics (10%) are removed from the bin-average process. The bin-averaged I-V characteristic is constructed from a time interval window of 0.5 ms and utilizes a "running" or "floating" window, when we move the 0.5 ms window (10 I-Vs) with a 0.05 ms step (1 I-V). This generates results which are also less sensitive to extremes. For better statistics 3 discharges were used for calculation of the mean value and standard deviation of the final α_{BPP} (see Fig. 8).

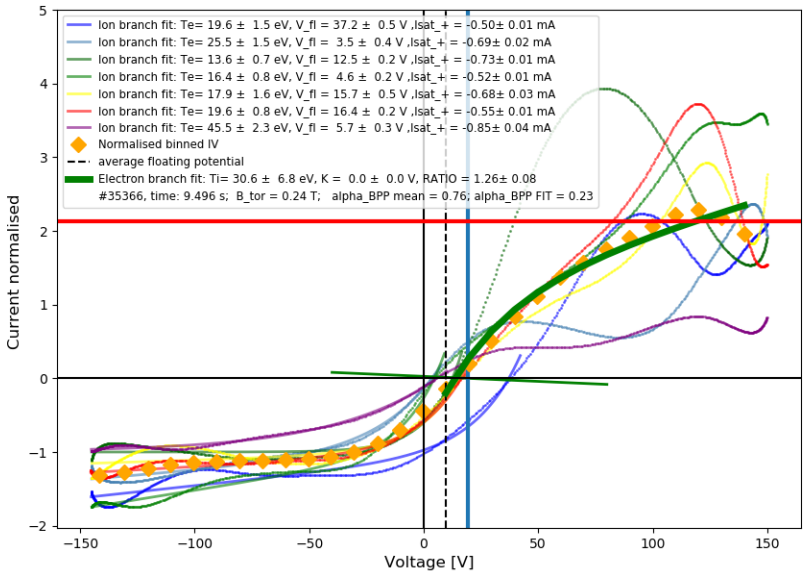

Figure 7: The 4-parameter fit (4) (green) of the bin-averaged I-V characteristics (orange). The black dashed line represents the average floating potential. The green line is a linear fit of second derivative of the bin-averaged I-V characteristic on the voltage applied, used for locating the plasma potential (blue line). The mean of saturated part of electron branch (red horizontal line) is the first estimate of electron to ion saturation current ratio.

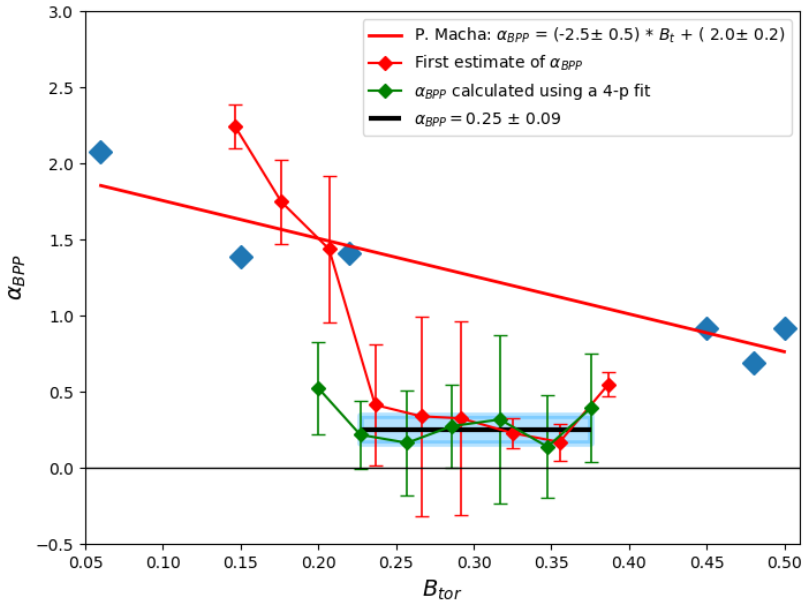

Figure 8: The resulting coefficient $\alpha_{\mathrm{BPP}} = 0.25 \pm 0.09$ (black line) was found as a mean of smooth (bin-averaged over 0.03 T) results gathered from 3 different discharges (green diamonds). The confidence interval of 1σ is indicated (blue area). All three discharges (#35347, #35352, #35366) were almost identical, with BPP biased with -150V to +150 V at 10 kHz sweeping frequency. The first estimates of the coefficient are shown (red diamonds). The previously found calibration dependency constructed form Fig. 6 is shown for comparison (blue diamonds, red line).

4. Ion and electron temperature measurements

Now that we have found the calibration coefficient of ball-pen probe we can proceed to fitting of the electron branch using a 4-parameter fit and a cutoff refitting routine, described in the previous report. An example of such fit is shown on Fig. 9

In order to create a temporal evolution of ion temperature with defined level of uncertainty we set filtering criteria as follows:

$$T_{\mathrm{i,err}}/T_{\mathrm{i}} > 0.6,$$
$$V_{\mathrm{p,err}}/V_{\mathrm{p}} > 0.6,$$
$$T_{\mathrm{i}} < (V_{\mathrm{peak}} - V_{\mathrm{p}})/1,$$

where $V_{\mathrm{peak}} = 150$ V is the peak value of voltage applied on the BPP. The resulting temporal evolution is shown on Fig. 17, 11 and 12.

We can now construct the radial profile of similar discharges at different radial positions using .

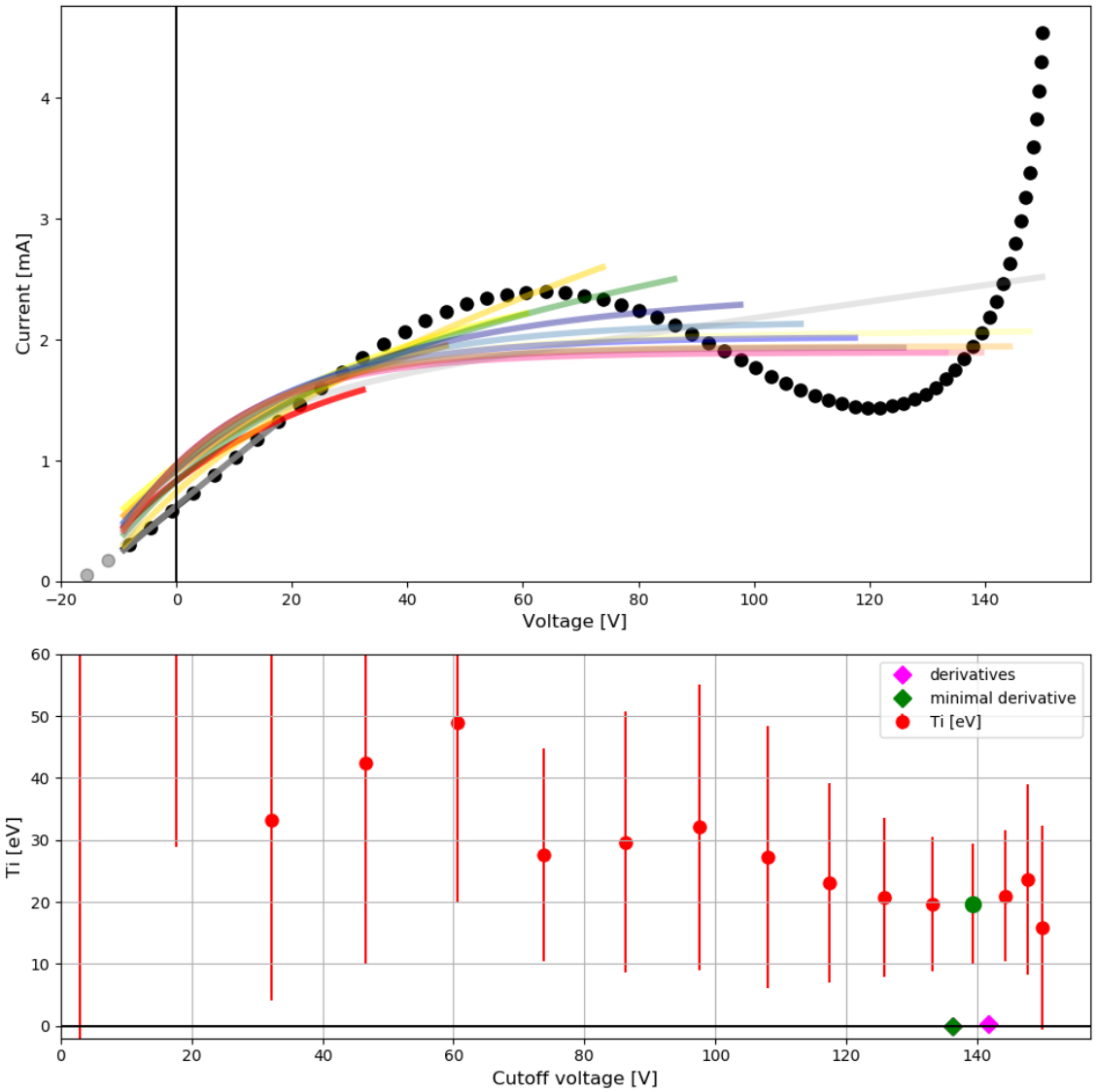

Figure 9: An example of a 4-parameter fit using a cutoff refitting routine.

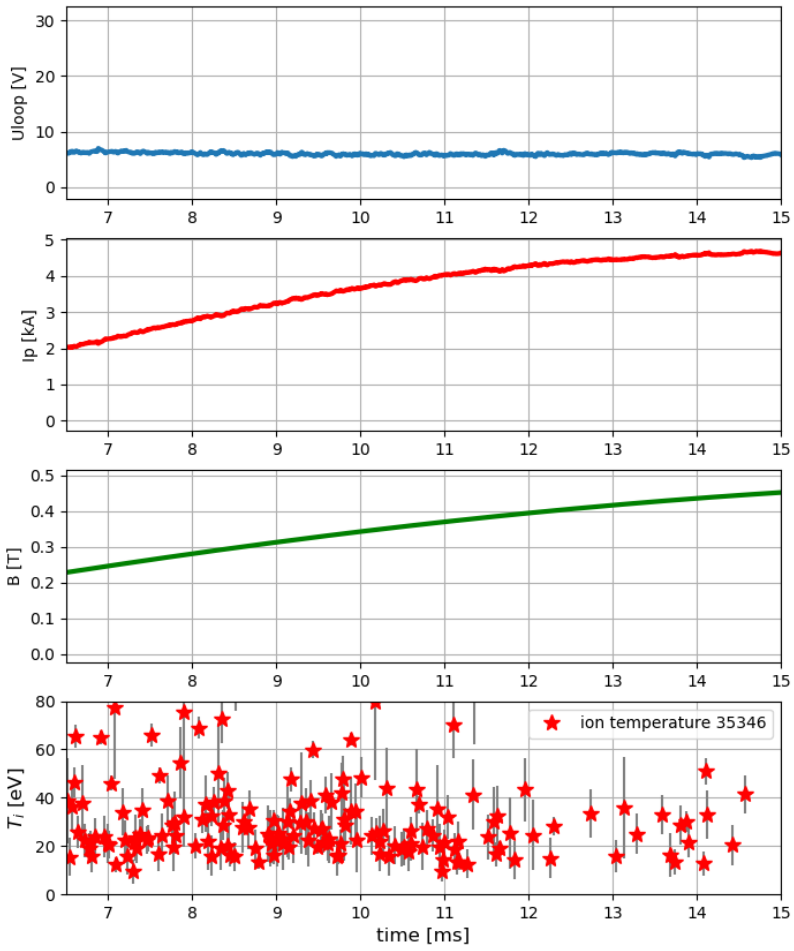

Figure 10: The temporal evolution of T_{i}, #35346, $R = 60$ mm

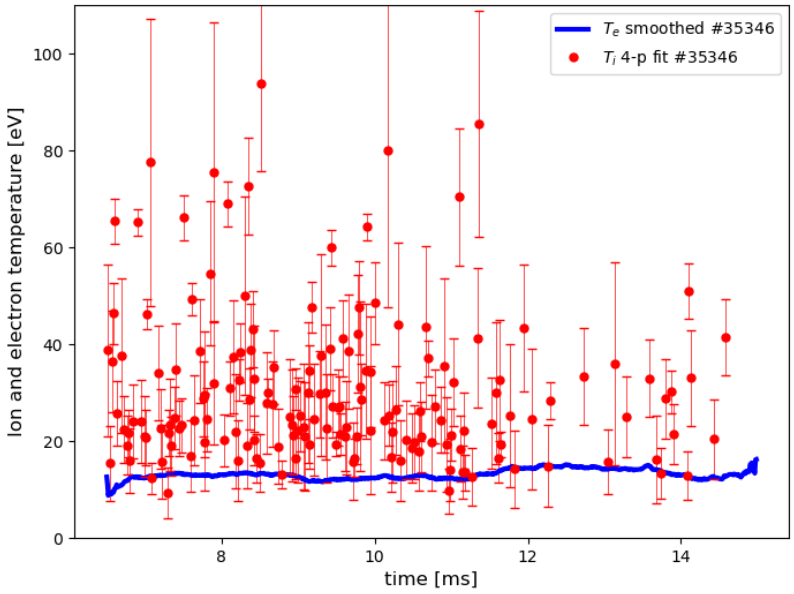

Figure 11: Detailed view of temporal evolution of T_i, #35346, $R = 60$ mm.

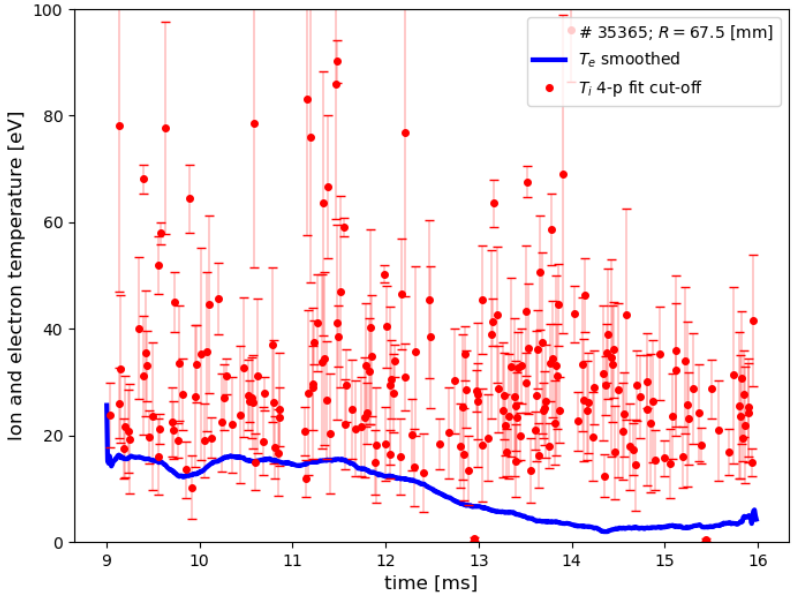

Figure 12: Detailed view of temporal evolution of T_i, #35365, $R = 67.5$ mm.

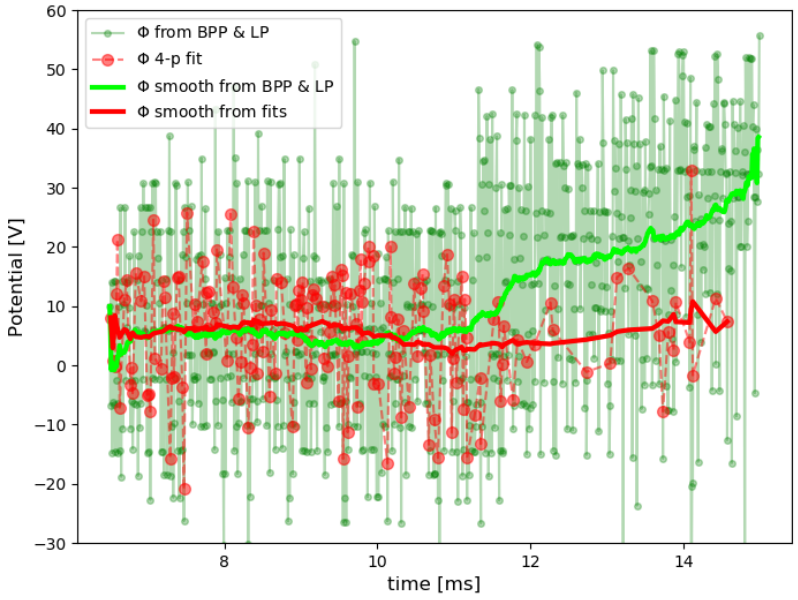

Figure 13: Comparison of the plasma potential calculated from 4-parameter fit and direct measurement of plasma potential, #35346, $R = 60$ mm

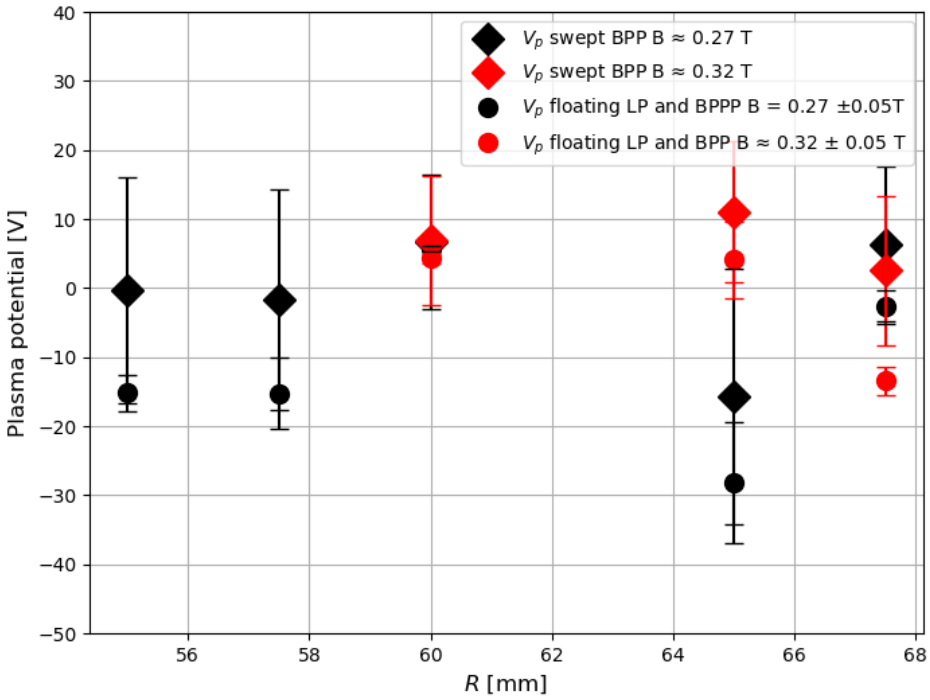

Figure 14: The radial profile of V_p obtained from fits and direct measurements.

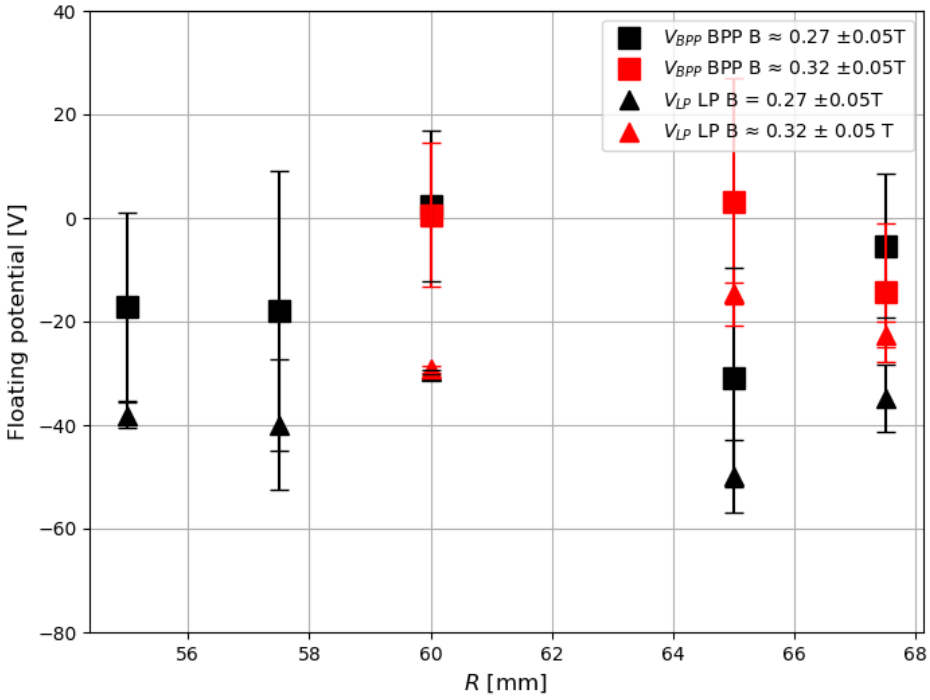

Figure 15: The radial profile of V_{fl} obtained from direct measurements with floating Langmuir probe and from I-V characteristics of BPP.

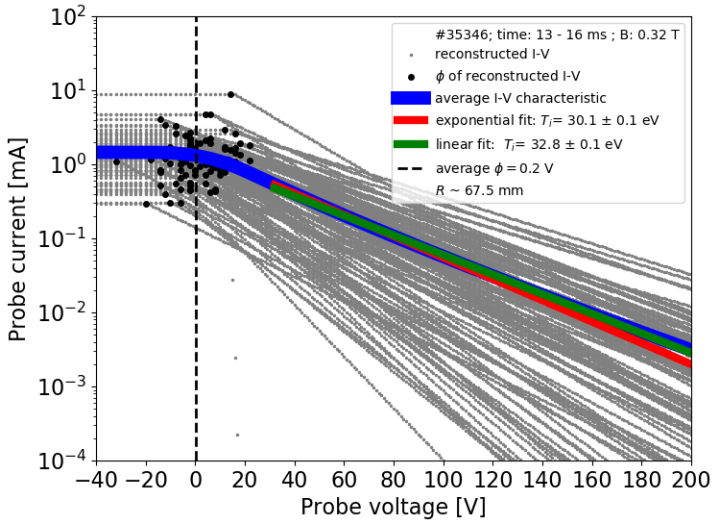

Figure 16: An example of synthetic RFA-like I-V characteristic.

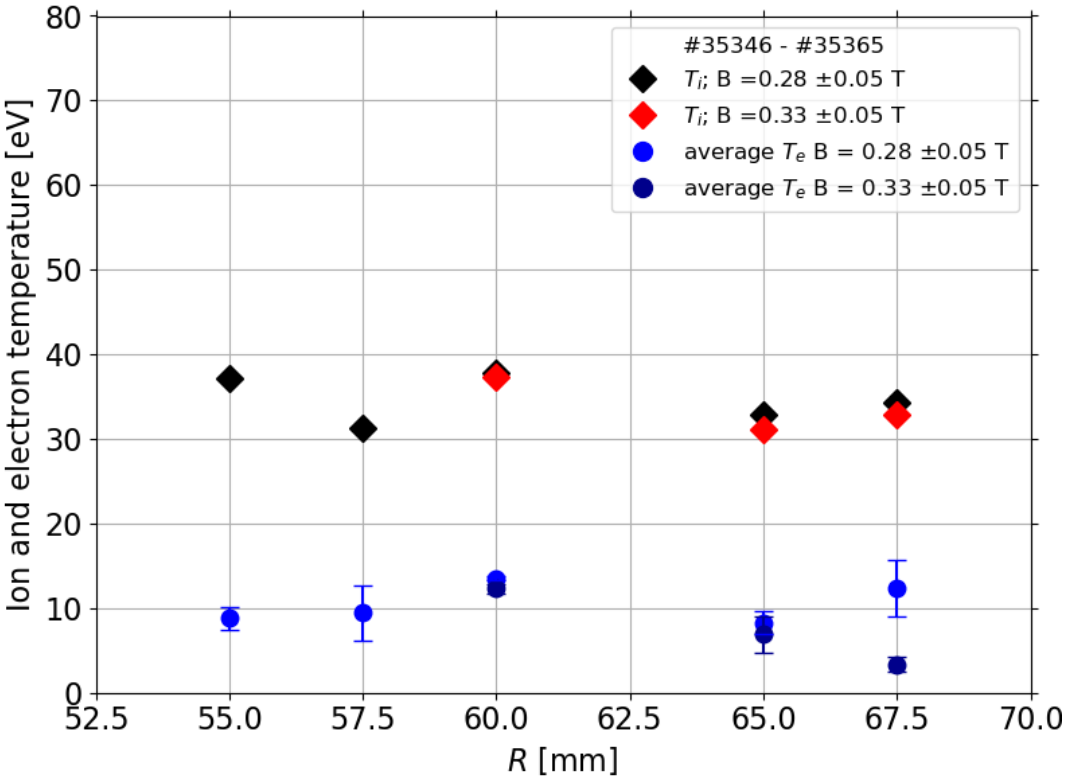

Figure 17: The radial profile of T_i obtained from linear fit of an "average" RFA-like I-V characteristics. Values of $T_\mathrm{i} > 5 * T_\mathrm{e}$ [eV] were not taken into construction of synthetic I-V characteristics, due to resulting significant overestimation of RFA T_i results.

5. Conclusion

In this report we have revised the previous results from most recent experimental campaign (4.2.2021) at tokamak GOLEM. A calibration constant was found for measurements with BPP as $\alpha_{\mathrm{BPP}} = 0.25 \pm 0.09$, which can be applied if the toroidal magnetic field reaches at least 0.25 T.

The validity of the calibration constant obtained was verified by comparison of the plasma potential obtained form 4-parameter fit (analytical function requires α_{BPP} given) and the direct measurement of the plasma potential using floating Langmuir probe and floating potential of BPP (found from BPP I-V characteristics).

The location of a separatrix is unclear due to fluctuation in plasma parameters and low spatial resolution obtained. One could make an educated guess that separatrix is located aproximatelly at $R = 62$ mm as can be seen form radial profiles of plasma potential an also radial profiles of floating potentials of both probes.

We have shown an example of the improved fitting approach (cutoff fitting), which significantly increases the yield of successfully fitted plasma parameters.

As can be seen on Fig. 12, during some discharges some unexpected changes of plasma parameters can occur. We do not know the exact reason for this behaviour.

The resulting temporal evolutions and the slow radial profiles indicate that the typical ratio $T_{\mathrm{i}}/T_{\mathrm{e}} \approx 3$ during the whole discharge. T_{i} values with significantly higher temperature are not correctly obtained values, but rather correspond to highly unsaturated I-V characteristics (possibly caused by impurities). The low energy (background) ions were not observed in this campaign. Possible reason is the low effective signal or the fact that $T_{\mathrm{i}} < 10$ eV do not occur at radial positions $R < 67.5$. In order to validate these results repeated experiment is required. Possible improvement can be done by using short coaxial cables connecting the fast swept probes to the DAS. The high DAS sampling frequency in combination with short cables would enable us to reach sweeping frequency even 100 kHz, an cutting-edge temporal resolution for ion temperature measurements of turbulent structures.